PEM Fuel Cell System Power Control based on a Feedback-Linearization Approach

Martin Schultze and Joachim Horn
Institute for Control Engineering, Helmut-Schmidt-University Hamburg

Abstract— **Polymer electrolyte membrane (PEM) fuel cell systems are highly efficient energy converters. Besides electrical power, low oxygen concentration cathode exhaust gas, water and heat are the byproducts if fed with pure hydrogen gas. So, this technology has become very attractive for the use on aircraft where it is investigated as replacement for the auxiliary power unit that is currently used for electrical power generation. Hence, controlling the fuel cell system for electrical power is a central topic. The electrical power output, however, is nonlinearly dependent on stack temperature, gas pressure, membrane humidity and stack current that is being drawn.**

This study deals with the controls of electrical power of an air and hydrogen fed self-powered fuel cell system. For controller design the nonlinear polarization curve is approximated by a linear current-voltage-characteristic. Based on a feedback-linearization approach a nonlinear control law for fuel cell system power is presented and implemented in a nonlinear fuel cell system simulation model. Even though the polarization curve is a linear approximation, the nonlinear control law leads to a fast response and zero steady state error.

I. Introduction

For aviation applications the fuel cell technology is investigated regarding to its multifunctional use. One aspect is the utilization of oxygen depleted cathode exhaust air (ODA) for kerosene tank inerting [1] if the oxygen content is close to or lower than 10% (vol.) [2]. Another and certainly the main aspect of the multifunctional use is electrical power generation. So far, an auxiliary power unit (APU) generates the electrical power consumed by the aircraft during ground operations. The APU, however, is a considerable source of noise and green house gases as it combusts kerosene. Replacing the APU by a hydrogen-gas fed PEM fuel cell system can significantly reduce these pollutants. Among the different types of fuel cells [3], PEM fuel cells are the most suitable ones for dynamic applications. Nonetheless, proper fuel cell system operation such as a well humidified membrane or a proper supply of reactant gases and well kept gas pressure is central for a maximum fuel cell lifetime [3]. In this study a self-powered evaporation cooled Intelligent Energy® PEM fuel cell system (FCS) as described in [4] is used. Proper fuel and air supply as well as system cooling is managed by an integrated fuel cell system controller.

The fuel cell system is connected to an ohmic electrical load that can be adjusted such that it draws a current as requested by an external reference. A schematic of the FCS connected to the load is shown in figure 1 and depicts the fuel cell system components and electrical connections.

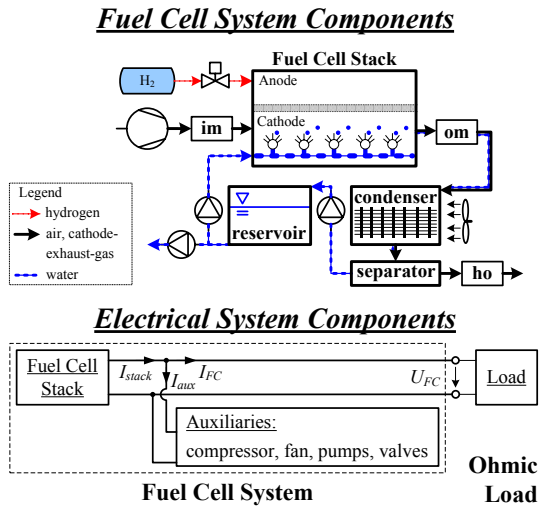

Fig. 1. The fuel cell system (FCS) consists of a stack, compressor, water reservoir, condenser, separator, valves, pumps and fans (top); it is connected to a load: stack current is partly used for internal power supply (bottom)

Simulation models reported of in the literature represent either convection cooled systems [5] or assume a constant stack temperature [6] or are used to investigate phenomena inside the fuel cell stack. For the system considered here, temperature is very important. Furthermore, the internal fuel cell system controls are mimicked to resemble the real system behavior. The simulation model in this study is an adapted combination of the models reported of in [7] and [8] and is briefly outlined in section Simulation Model.

For the use as an electrical power generator, the fuel cell system has to deliver electrical power as requested. For fuel cell system controls various controller architectures have been proposed in the literature. [6], [9] and [10] propose linear feedback controllers to control for the gas and fuel mass flows and pressure differences in the stack. In [11] an LQG regulator approach was used to control for proper air supply. In [12] and [13] model predictive control was favored to control for the air flow and fuel cell electrical power, respectively. [14] and [15] propose a nonlinear controller based on a feedback-linearization approach to

Manuscript received January 30, 2012. This study as part of the project "cabin technology and multifunctional fuel cell systems" has been supported by Airbus and the German Federal Ministry of Education and Research (support code: 03CL03A).

Martin Schultze and Joachim Horn are with the Institute for Control Engineering, Helmut-Schmidt-University Hamburg, Holstenhofweg 85, D-22043 Hamburg, Germany (e-mail: Martin.Schultze@hsu-hh.de, Joachim.Horn@hsu-hh.de).

control for gas mass flow and pressure difference in the stack. For the electrical power control of a self-powered fuel cell system with internal controls a nonlinear controller is proposed based on a feedback-linearization approach.

This paper is organized as follows: The simulation model is described in section Simulation Model. The proposed nonlinear controller for fuel cell system electrical power is described in section Controller Design. The controller is implemented and tested with the nonlinear fuel cell system simulation model. Simulation results are shown in the last section Simulation Results.

II. SIMULATION MODEL

The system simulation model comprises models of the self-powered Intelligent Energy® fuel cell system, the internal FCS controller and the ohmic electrical load to which the fuel cell system is directly connected. The electrical power provided by the fuel cell stack is partly taken to power auxiliary components such as compressor, pumps and valves as shown in figure 1. The real fuel cell system comprises a buffer battery [8, 10] that is used to power the auxiliaries during startup and load transients. Here, battery and its charging-dynamics are not considered.

A. Fuel Cell System Model

The fuel cell system model as described in [7] comprises an evaporation cooled fuel cell stack, a compressor model for air supply and a model of the condenser. Condensate is separated from the gas flow and pumped into a cooling water tank to be injected for stack cooling. The fuel cell system controller [4] limits the current being allowed to be drawn based on compressor and internal states. So, the overall system dynamics is limited mainly by compressor dynamics. Inlet air is modeled as a dry and ideal gas consisting of 21% (vol.) oxygen and 79% (vol.) nitrogen.

Compressor Model

The compressor is modeled as a dc motor driving a blower [8]. The motor armature current I_A establishes very fast as compared to the rotational speed. Therefore, it is modeled as static [6]. The compressor mass flow W_{cp} is coupled to the rotational speed ω of the dc motor by the blower constant b_{cp}. The model equations are as follows.

$$J\frac{d\omega}{dt} = K_c I_A - k_d\omega \tag{1}$$

$$I_A = \frac{1}{R_A}(U_A - K_c\omega) \tag{2}$$

$$W_{cp} = b_{cp}\omega \tag{3}$$

R_A is the dc motor resistance and J the total moment of inertia of motor and fan. The motor input voltage is U_A, which is limited to 5-24V. Motor rotation causes the back-electromotive force $K_c\omega$. K_c is the torque and back emf constant. Linear friction is modeled by the damping constant k_d. The compressor's consumption of electrical power P_{cp} (4) is given by armature current and motor input voltage U_A.

$$P_{cp} = U_A I_A \tag{4}$$

The air mass flow W_{cp} leaving the compressor is PI-controlled (5) with a mass flow reference W_{cp}^{ref} and an antiwindup circuit to avoid integrator windup with $U_{sat}=24V$ for $U_A>24V$, $U_{sat}=5V$ for $U_A<5V$ and $U_{sat}=U_A$ otherwise.

$$\begin{aligned} U_A &= k_p\left(W_{cp}^{ref} - W_{cp}\right) + k_i\int W_{cp}^{ref} - W_{cp} - U_{awindup}\,dt \\ U_{awindup} &= U_A - U_{sat} \end{aligned} \tag{5}$$

Auxiliary Components

Auxiliary power P_{aux} is the sum (6) of compressor power P_{cp} and consumption of auxiliary components modeled by a constant P_{const}. Auxiliaries are connected to the fuel cell by an internal power supply [8] that transforms auxiliary power into an auxiliary current I_{aux_total} with an efficiency of approximately 95%. U_{FC} is the fuel cell stack voltage. As [10] proposes a low pass filter with cutoff frequency 0.5 Hz, whose corresponding time constant is T_{aux}, is implemented to avoid sharp transients in auxiliary current acting on the fuel cell. High frequency parts of the total auxiliary current I_{aux_total} are taken from the buffer battery, whereas low frequency parts convert to the auxiliary current I_{aux} (8). The battery current would be given as I_{aux_total} - I_{aux}.

$$P_{aux} = P_{cp} + P_{const} \tag{6}$$

$$I_{aux\_total} = \frac{P_{aux}}{U_{FC}\cdot 0.95} \tag{7}$$

$$T_{aux}\frac{dI_{aux}}{dt} = -I_{aux} + I_{aux\_total} \tag{8}$$

Inlet and Outlet Manifold Model

Manifold mass m_{im} and pressure p_{im} (9) are gained by a mass balance and pressure differential equation ($\gamma=1.4$ [6]). Mass flow W_{ca_in} of dry air exiting the inlet manifold is modeled by a linear nozzle equation with constant k_{im} and the pressure difference of manifold and cathode pressure p_{ca}. $T_{im} = (p_{im}V_{im})/(m_{im}R_{air})$ is the manifold temperature with the manifold volume V_{im} and air gas constant R_{air}. In the outlet manifold vapor mass flow is obtained by the water loading (11) of the dry gas mass flow. Water loading depends on gas pressure p_i, relative humidity ϕ_i and temperature T_i, which defines the saturation vapor pressure [16] (12).

$$\frac{dm_{im}}{dt} = W_{cp} - W_{ca\_in},\quad \frac{dp_{im}}{dt} = \frac{\gamma R_{air}}{V_{im}}\left(T_{cp}W_{cp} - T_{im}W_{ca\_in}\right) \tag{9}$$

$$W_{ca\_in} = k_{im}\left(p_{im} - p_{ca}\right) \tag{10}$$

$$X_i = \frac{\phi_i p_v^{sat}(T_i)}{p_i - \phi_i p_v^{sat}(T_i)}\frac{R_{air}}{R_v} \tag{11}$$

$$p_v^{sat} = \exp\left(17.2799 - \frac{4102.99}{\vartheta + 237.431}\right)0.611657\times 10^3 \tag{12}$$

Mass flows of water vapor W_{v_ca}, oxygen depleted air W_{oda_ca} and liquid water W_{w_ca} are supplied to the outlet manifold at stack temperature T_{st}. The manifold is considered perfectly insulated. Mass flows W_{v_om}, W_{oda_om} and W_{w_om} exit directly into the condenser and are governed by a nonlinear nozzle equation (13) and (14) with C_{hex} being the conductivity and φ the nonlinear flow function [6]. Flow

of liquid water leaving the manifold is modeled as $W_{w\_om}=\delta_l W_{om} m_{w\_om}$ [7] with liquid-mass m_{w_om}, and a constant δ_l. Partial pressures of dry gas p_{oda_om} and vapor p_v are gained by mass-balance and the ideal gas law (14) with manifold volume V_{om} and the vapor gas constant R_v. ODA is taken as air with gas constant R_{air}. Condensation is assumed happening instantaneously leading to condensate mass m_{cond} and liquid mass m_w. Total gas pressure in the outlet manifold is obtained by the sum of gas and vapor partial pressures (16). Condenser outlet manifold is modeled equivalently to the outlet manifold with exiting mass flow W_{ho} governed by a linear nozzle equation similar to (10) with constant k_{ho} and difference of manifold p_{ho} and ambient pressure p_{amb}.

$$W_{om} = \varphi\left(\frac{p_{ho}}{p_{om}}, b_{hex}\right) C_{hex}\, p_{om} \tag{13}$$

$$\frac{dp_{oda\_om}}{dt} = \frac{T_{st} R_{air}}{V_{om}}\left(W_{oda\_ca} - W_{oda\_om}\right),\ W_{oda\_om} = \frac{1}{1+X_{om}} W_{om}$$

$$\frac{dp_{v\_om}}{dt} = \frac{T_{st} R_v}{V_{om}}\left(W_{v\_ca} - W_{v\_om}\right),\qquad W_{v\_om} = \frac{X_{om}}{1+X_{om}} W_{om}$$

$$m_w = m_{cond} + \int W_{w\_ca} - W_{w\_om}\, dt \tag{14}$$

$$m_{cond} = \begin{cases} 0 & , p_v \le p_v^{sat} \\ \frac{V}{R_v T}\left(p_v - p_v^{sat}\right) & , p_v > p_v^{sat} \end{cases} \tag{15}$$

$$p_{om} = p_{oda\_om} + \begin{cases} p_{v\_om} & , p_{v\_om} \le p_v^{sat} \\ p_v^{sat} & , p_{v\_om} > p_v^{sat} \end{cases} \tag{16}$$

Condenser, Separator and Catchpot Model

The condenser is modeled by the εNTU method [17]. The heat flow $\dot{Q}_{hex} = \varepsilon_{hex} \cdot \min(\dot{Q}_{fan}^{\max}, \dot{Q}_{flow}^{\max})$ is governed by the effectiveness ε_{hex} [7] and the maximum heat flows (17). Condenser pressure p_{hex} is modeled as average of outlet and condenser-outlet manifold pressures. W_i are mass flows of cooling air, ODA, water and vapor, c_i heat capacities, h_0 enthalpy of evaporation and ϑ temperatures of stack and ambient in °C. Relative humidity at the condenser exit is 100%. Mass flows of vapor W_v and liquid water W_w at the condenser exit are governed by (18) with the water loading X_{cond}. The nonlinear energy balance (19) leads to the condenser exit temperature with $\vartheta_{cond} = k_{p\_cond} \int e\, dt$.

$$\begin{aligned} \dot{Q}_{fan}^{\max} &= W_{air} c_{air}\left(\vartheta_{st} - \vartheta_{amb}\right) \\ \dot{Q}_{flow}^{\max} &= W_{oda\_om} c_{air}\left(\vartheta_{st} - \vartheta_{amb}\right) + W_{w\_om} c_w \vartheta_{st} - W_w c_w \vartheta_{amb} \\ &\quad + W_{v\_om}\left[h_0 + c_v \vartheta_{st}\right] - W_v\left[h_0 + c_v \vartheta_{amb}\right] \end{aligned} \tag{17}$$

$$W_v = X_{cond} W_{oda\_om},\qquad W_w = W_{w\_om} + W_{v\_om} - W_v \tag{18}$$

$$\begin{aligned} e &= W_{oda\_om} c_{air}\left(\vartheta_{st} - \vartheta_{cond}\right) + W_{w\_om} c_w \vartheta_{st} - W_w c_w \vartheta_{cond} \\ &\quad + W_{v\_om}\left[h_0 + c_v \vartheta_{st}\right] - W_v\left[h_0 + c_v \vartheta_{cond}\right] - \dot{Q}_{hex} \end{aligned} \tag{19}$$

The cyclone separates liquid water from the gas stream. Its efficiency is $\eta_{cyclone}$ [7]. Water gathers in a vessel where it is pumped from into the catchpot as $W_{cpump} = k_{p\_cpump} m_{cyc}$. The mass m_{cyc} in the vessel is gained by a mass balance (20).

$$\frac{dm_{cyc}}{dt} = \eta_{cyclone} W_{w,out} - W_{cpump} \tag{20}$$

The catchpot is filled by W_{cpump} and emptied by the drainage mass flow W_{dpump} and the cooling water injection mass flow W_{inject}. The catchpot water mass m_{cpot} as well as temperature T_{cpot} are governed by mass conservation and an energy balance (21). The drainage pump is operated by a 2-point-control to maintain a filling level of 69.5-70.5%.

$$\begin{aligned} \frac{dm_{cpot}}{dt} &= W_{cpump} - W_{inject} - W_{dpump} \\ m_{cpot}\frac{dT_{cpot}}{dt} &= W_{cpump} T_{cond} - \left(W_{inject} + W_{dpump}\right) T_{cpot} - \frac{dm_{cpot}}{dt} T_{cpot} \end{aligned} \tag{21}$$

Injection Model and Fuel Cell Stack Electrical Model

The injection pump injects the cooling water mass flow W_{inject} from the catchpot into the fuel cell stack cathode. W_{inject} is coupled to the stack current being drawn [7].

The stack voltage $U_{FC} = n_{cells} U_{cell}$ is the sum of all n_{cells} cell voltages. Cell voltage is modeled as $U_{cell} = U_{rev} - \eta_{act} - \eta_\Omega$ (22) with reversible cell voltage U_{rev}, activation loss η_{act} [18] and ohmic loss η_Ω [19]. The membrane thickness is given by d_m and the active surface area by A_{sfc}. Parameters $\zeta_1, \ldots \zeta_4$, b_1 and b_2 have been identified experimentally [7].

$$\begin{aligned} U_{rev} &= 1.229 - 0.85\cdot 10^{-3}\left(T_{st} - 298.15\right) + 4.3\cdot 10^{-5} T_{st}\left(\ln\tfrac{p_{H2}}{p_0} + \tfrac{1}{2}\ln\tfrac{p_{O2}}{p_0}\right) \\ \eta_{act} &= \zeta_1 + \zeta_2 T_{st} + \zeta_3 T_{st}\ln\left(p_{O2} e^{(498/T_{st})}/5.08\cdot 10^{-6}\right) + \zeta_4 T_{st}\ln\left(I_{stack}\right) \\ \eta_\Omega &= \frac{d_m}{\left(b_1\lambda_m - b_2\right)} e^{-1268\left(1/303 - 1/T_{st}\right)} \frac{I_{stack}}{A_{sfc}} \end{aligned} \tag{22}$$

Fuel Cell Stack Thermal and Memebrane Model

An energy balance (23) using chemical energy of hydrogen (HHV) and stack electrical energy, a stack water and vapor energy balance as well as heat transfer to surroundings with transfer coefficient R_{sa} and stack heat capacity C_{st} lead to the fuel cell stack temperature T_{st} [7].

$$\begin{aligned} \dot{Q}_{flow} &= W_{w\_ca} c_w \vartheta_{st} + W_{v\_ca}\left[h_0 + c_v \vartheta_{st}\right] - W_{inject} c_w \vartheta_{cpot} \\ C_{st}\frac{dT_{st}}{dt} &= \left(1.48\, n_{cells} - U_{FC}\right) I_{stack} - R_{sa}\left(T_{st} - T_{amb}\right) - \dot{Q}_{flow} \end{aligned} \tag{23}$$

Membrane material is Nafion®. The membrane water mass flow W_{mem} (24) is caused by gradient driven diffusion and electro-osmotic drag from anode to cathode [19]. Diffusion constant D_{diff} depends on the membrane hydration λ_{mem} and stack temperature (25). The membrane water activity a_{mem} is modeled as the average between cathode and anode water activity [19] (with j=*mem, ca, an*).

$$W_{mem} = A_{sfc} M_w n_{cells}\left(\lambda_{mem}\frac{2.5}{22}\frac{I_{stack}}{A_{sfc}F} - \frac{\rho_{dry}}{M_{dry}} D_{diff}\frac{\lambda_{ca} - \lambda_{an}}{d_m}\right) \tag{24}$$

$$D_{diff} = e^{2416\left(1/303 - 1/T_{st}\right)}\left(2.563 - 0.33\lambda_{mem} + 0.0264\lambda_{mem}^2 - 0.000671\lambda_{mem}^3\right)\cdot 10^{-6}$$

$$\lambda_j = \begin{cases} 0.043 + 17.81 a_j - 39.85 a_j^{\,2} + 36.0 a_j^{\,3} & 0 < a_j \le 1 \\ 14 + 1.4\left(a_j - 1\right) & 1 < a_j \le 3 \end{cases} \tag{25}$$

Fuel Cell Stack Anode and Cathode Model

Anode pressure $p_{an} = p_{H2} + p_{v\_an}$ is the sum of H_2 and vapor partial pressures and is governed by (26) and the ideal gas law with R_{H2} being the hydrogen gas constant. In operation a mass flow $W_{H2rct} = (M_{H2} I_{stack} n_{cells})/(2F)$ of hydrogen reacts. The stack is operated dead-ended and the system behavior is mimicked by a proportional controller for anode pressure p_{an} with hydrogen inlet mass flow W_{H2}, anode reference pressure p_{an_ref} and controller gain $k_{p\_ctrl\_an}$.

$$\frac{dm_{w\_an}}{dt} = -W_{mem} \text{ and } \frac{dp_{H2}}{dt} = \frac{T_{st}R_{H2}}{V_{an}}\left(W_{H2} - W_{H2rct}\right) \quad (26)$$

$$W_{H2} = k_{p\_ctrl\_an}\left(p_{an\_ref} - p_{an}\right) \quad (27)$$

Condensation is modeled happening instantaneously [6] if the vapor pressure exceeds saturation vapor pressure. The mass of condensate is given as the difference of liquid water and vapor mass $m_{cond} = m_w - m_v$. The vapor mass is obtained by a mass balance and cannot exceed $m_v^{sat} = p_v^{sat}V/(R_vT_{st})$. The cathode inlet mass flows of oxygen and nitrogen are governed by the mass fractions x_{O2} and x_{N2}. The cathode exit mass flow W_{ca} is modeled as a 3-phase-flow (28) and is governed by a linear nozzle equation similar to (10) with constant k_{ca} and pressure difference p_{ca}-p_{om}. Liquid water mass flow W_{w_ca} is modeled similarly to the outlet manifold. Cathode pressure $p_{ca} = p_{O2} + p_{N2} + p_{v\_ca}$ is the sum of oxygen, nitrogen and vapor partial pressures and is governed by mass conservation (29) and the ideal gas law [7]. In operation a mass flow $W_{O2rct} = (M_{O2}I_{stack}n_{cells})/(4F)$ of oxygen is consumed and $W_{H2Orct} = (M_{H2O}I_{stack}n_{cells})/(2F)$ of water is generated. Condensation happens instantaneously.

$$\begin{bmatrix} W_{O2\_cp} \\ W_{N2\_cp} \end{bmatrix} = \begin{bmatrix} x_{O2} \\ x_{N2} \end{bmatrix} W_{cp} \text{ and } \begin{bmatrix} W_{O2\_ca} \\ W_{N2\_ca} \\ W_{v\_ca} \end{bmatrix} = \frac{1}{1+X_{CA}} \begin{bmatrix} \frac{m_{O2}}{m_{O2}+m_{N2}} \\ \frac{m_{N2}}{m_{O2}+m_{N2}} \\ X_{CA} \end{bmatrix} W_{ca} \quad (28)$$

$$\frac{dm_{w\_ca}}{dt} = W_{mem} + W_{inject} + W_{H2Orct} - W_{v\_ca} - W_{w\_ca} \quad (29)$$

$$\frac{dm_{O2}}{dt} = W_{O2\_cp} - W_{O2rct} - W_{O2\_ca}$$

$$\frac{dm_{N2}}{dt} = W_{N2\_cp} - W_{N2\_ca}$$

Internal Fuel Cell System Controls

As outlined in [4] the fuel cell system dynamics are limited by either the slow compressor dynamics or the dynamics of the remaining system if the compressor already runs sufficiently fast. As further shown in [4] the remaining system dynamics allow for an almost linear current slope of about 100A/s. To mimic this behavior a reference signal I_{FCref} is generated. I_{FCref} is the current that actually can be drawn from the fuel cell system by an electrical load. In this system configuration a current request I_{FCreq} must be sent to the fuel cell system controller, which subsequently adjusts the compressor to deliver the correct air mass flow. Air mass flow reference signal (30) is generated based on stoichiometry request λ_{ref}, current request I_{FCreq} and auxiliary current I_{aux_m} measured by a current sensor modeled as a first order system with time constant 0.01s.

$$W_{cp}^{ref} = \left(M_{O2} + \frac{0.79}{0.21}M_{N2}\right)\frac{n_{cells}}{4F}\lambda_{ref}\left(I_{FCreq} + I_{aux\_m}\right) \quad (30)$$

The compressor has a minimum speed and therefore delivers a minimum air mass flow. In that case and if the compressor already runs sufficiently fast, the system dynamics are limited by the remaining fuel cell system dynamics such as fuel supply, cooling etc. To limit the dynamics to 100A/s a limiter model (31) is implemented.

$$\frac{dI_{FC\_ltr}}{dt} = \int i_{sat}dt \text{ and } i_{sat\_in} = 10^3\left(I_{FCreq} - I_{FC\_ltr}\right) \quad (31)$$

with $i_{sat} = 100A/s$ for $i_{sat\_in} > 100A/s$ and $i_{sat} = i_{sat\_in}$ otherwise. The fuel cell current reference signal I_{FCref} is calculated based on the minimum (32) of the limiter output and the reference signal (33) based on the compressor air mass flow W_{cp} and constant stoichiometry request λ_{ref}.

$$I_{FCref} = \min\left(I_{stack\_ref} - I_{aux\_m}, I_{FC\_ltr}\right) \quad (32)$$

$$I_{stack\_ref} = \frac{4F}{\left(M_{O2} + \frac{0.79}{0.21}M_{N2}\right)n_{cells}\lambda_{ref}}W_{cp} \quad (33)$$

The constants M_{O2} and M_{N2} define the molar mass of oxygen and nitrogen, respectively [16]. Figure 3 shows a schematic of the internal system controller architecture. The stack current (34) that actually is being drawn is the sum of auxiliary current I_{aux} and the fuel cell current I_{FC}.

$$I_{stack} = I_{aux} + I_{FC} \quad (34)$$

B. *Electrical Load Model*

The ohmic electrical load draws a current as requested by the reference signal I_{Lreq}. An internal load controller very quickly adjusts the internal resistance R_L according to the voltage across the load. The load model is a first order transfer function with time constant T_L to prevent numerical problems. Fuel cell current drawn I_{FC} is the load current I_L.

III. Controller Architecture

The objective of the electrical power controller is to deliver the electrical power that is requested. The fuel cell system electrical power $P_{FC} = U_{FC}I_{FC}$ is the product of fuel cell stack voltage U_{FC} and fuel cell system current I_{FC}.

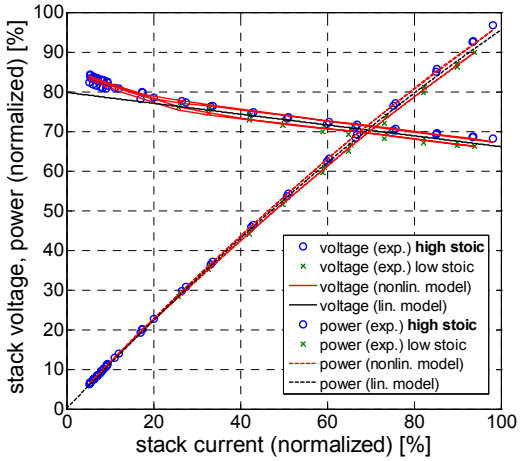

Fig. 2. Polarization curve and electrical power curve of the fuel cell stack [7] showing experimental data, the nonlinear and linear voltage model

As can be seen in (22) the fuel cell voltage depends on stack current, temperature, gas pressure and membrane humidity. So, the stack power P_{FC} nonlinearly depends on these parameters as well. For this fuel cell system the membrane can be considered perfectly wet as liquid water is injected into the cathode such that the membrane is humidified simultaneously. Increasing stoichiometry leads to increasing cathode pressure. The influence of high and low stoichiometry can be seen in the polarization curve in figure 2. The stack voltage, however, is most importantly dependent on stack current as shown in figure 2.

Motivated by the almost linear slope of the polarization curve in the stack current region of 20-100% and as proposed by [20] the polarization curve is approximated as a linear curve for controller design. For the linear curve the curves for high and low stoichiometry have been averaged in the region of interest. The stack voltage U_{st} is obtained by open circuit voltage U_0, resistance R and stack current I_{stack} as $U_{st} = U_0 - RI_{stack}$. Electrical power is given by the product of voltage and fuel cell system current I_{FC} (35).

$$P_{FC} = U_{stack} I_{FC} = (U_0 - RI_{stack}) I_{FC} = (U_0 - RI_{stack})(I_{stack} - I_{aux}) \quad (35)$$

For the controller model the following states are defined $[x_1\ x_2\ x_3\ x_4\ x_5] = [I_{stack\_ref}\ I_{FC\_ltr}\ I_{aux}\ I_{stack}\ I_{FC}]$ with $x_4 = x_3 + x_5$ and $x_5 = min(x_1 - x_3, x_2)$ assuming an instantaneous electrical load such that $I_{stack} = I_{stack\_ref}$. The compressor model is approximated by a PT1 system with time constant T_{cp}. Compressor power is modeled static by the factor Z_{cp} and $(u + x_3)^2$ the input squared. The limiter is considered a first order time system with constant T_{ltr}. The simplified system model is as follows with system input u and output $y = (U_0 - Rx_4)x_5$.

$$\begin{bmatrix} \dot{x}_1 \\ \dot{x}_2 \\ \dot{x}_3 \\ \dot{x}_4 \\ \dot{x}_5 \end{bmatrix} = \begin{bmatrix} \frac{1}{T_{cp}}(-x_1 + x_3 + u) \\ \frac{1}{T_{ltr}}(-x_2 + u) \\ \frac{1}{T_{aux}}\left(-x_3 + \frac{P_{const}}{(U_0 - Rx_4)\eta} + \frac{Z_{cp}(u + x_3)^2}{(U_0 - Rx_4)\eta}\right) \\ \dot{x}_3 + \dot{x}_5 \\ \frac{d}{dt}\min(x_1 - x_3, x_2) \end{bmatrix} \quad (36)$$

In the approach of feedback-linearization [15] the output y is derived with respect to time until the input u appears.

$$\begin{aligned} \dot{y} &= (U_0 - Rx_4)\dot{x}_5 - R\dot{x}_4 x_5 = (U_0 - Rx_4)\dot{x}_5 - R(\dot{x}_5 + \dot{x}_3)(x_4 - x_3) \\ &= (U_0 - 2Rx_4 + Rx_3)\dot{x}_5 - Rx_5\dot{x}_3 \end{aligned} \quad (37)$$

The input u appears in the first derivative with respect to time of the output y as can be seen by $\dot{x}_5$ in (37). The nonlinear control law (38) with reference y_{ref} is as follows. With U_0 being ca. 160V, R being ca. 0.2Ω and a maximum stack current of 130A the denominator in (38) is greater than zero.

$$u = x_4 - x_3 + \frac{1}{U_0 - 2Rx_4 + Rx_3}(y_{ref} - y) \quad (38)$$

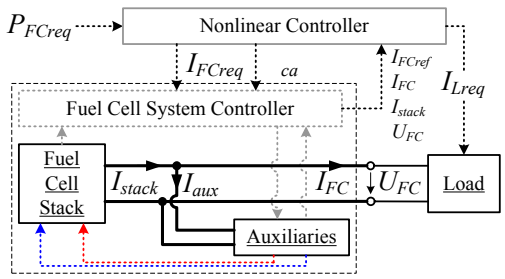

Fig. 3. Structure of the fuel cell system with the nonlinear controller

A schematic of the controller structure is shown in figure 3. The electrical power reference is P_{FCreq}. The current requested from the electrical load is $I_{Lreq} = I_{FCref}$ and the system input is the fuel cell current request $I_{FCreq} = u$. To show stability of this controller two cases have to be looked at. Firstly, when the compressor already runs sufficiently fast and the limiter prescribes the dynamics. Then, the fuel cell current I_{FC} equals the limiter output I_{FC_ltr} leading to $x_5 = x_2$. The auxiliary power drawn does not change as the compressor controller works within the saturation. The differential equations (36) and (37) and $x_5 = x_2$ lead to (39).

$$\dot{y} = \frac{(U_0 - 2Rx_4 + Rx_3)}{T_{ltd}}\left(\underbrace{-x_5 - x_3 + x_4}_{=0} + \frac{y_{ref} - y}{U_0 - 2Rx_4 + Rx_3}\right) - \underbrace{Rx_5\dot{x}_3}_{\delta_a} \quad (39)$$

$$\dot{y} = \frac{1}{T_{ltr}}(y_{ref} - y) - \delta_a$$

As the compressor controller works within the saturation, input u does not act on state x_3. Equation for x_3 turns to (40).

$$\dot{x}_3 = \frac{1}{T_{aux}}\left(-x_3 + \frac{P_{const} + Z_{cp}^*}{(U_0 - Rx_4)\eta}\right) \quad (40)$$

With $(U_0 - Rx_4)\eta$ being a positive number in the region of operation, (40) is asymptotically stable leading to δ_a going to zero and so leading to a steady state value $y = y_{ref}$. The second case is when the compressor limits the system dynamics. In this case the fuel cell current I_{FC} equals $I_{stack\_ref} - I_{aux}$ leading to $x_5 = x_1 - x_3$ and the stack current I_{stack} equals the stack current reference I_{stack_ref} leading to $x_1 = x_4$.

$$\dot{y} = \frac{(U_0 - 2Rx_4 + Rx_3)}{T_{cp}}\left(\underbrace{x_3 - x_1 - x_3 + x_4}_{=0} + \frac{y_{ref} - y}{U_0 - 2Rx_4 + Rx_3}\right) - \underbrace{(U_0 - Rx_4)\dot{x}_3}_{\delta_b}$$

$$\dot{y} = \frac{1}{T_{cp}}(y_{ref} - y) - \delta_b \quad (41)$$

Inserting the control law and equation for output y into the equation for x_3, the equation for this state is as follows.

$$\dot{x}_3 = \frac{1}{T_{aux}}\left(-x_3 + \frac{P_{const}}{(U_0 - Rx_4)\eta} + \frac{Z_{cp}}{(U_0 - Rx_4)\eta}\left[x_4 + \frac{y_{ref} - (U_0 - Rx_4)(x_4 - x_3)}{U_0 - 2Rx_4 + Rx_3}\right]^2\right)$$

Exploiting $\frac{U_0 - Rx_4}{U_0 - 2Rx_4 + Rx_3} \approx 1$ and $x_3 > 0$, the above equation simplifies to (42) resulting in inequality (43) for stability.

$$\dot{x}_3 = \frac{1}{T_{aux}}\left(-x_3 + \frac{1}{(U_0 - Rx_4)\eta}\left(P_{const} + Z_{cp}\left[\frac{y_{ref}}{U_0 - 2Rx_4 + Rx_3} + x_3\right]^2\right)\right) \quad (42)$$

$$x_3 < \frac{(U_0 - Rx_4)\eta}{Z_{cp}} - 2\frac{y_{ref}}{U_0 - 2Rx_4 + Rx_3} \quad (43)$$

With term $(U_0 - Rx_4)\eta > 100$ and a positive Z_{cp} being 0.05 or less and the maximum power reference [4], this inequality is satisfied over the entire fuel cell system operating region. As the state x_3 is stable δ_b is going to zero and therefore leads to a steady state value $y = y_{ref}$. Moreover, this nonlinear controller is robust against fuel cell voltage model uncertainties as can be shown by a voltage deviation ΔU on the fuel cell stack voltage U_{FC}.

$$\dot{y} = \frac{1}{T_{ltd}}\frac{(U_0 - 2Rx_4 + Rx_3 + \Delta U)}{U_0 - 2Rx_4 + Rx_3}(y_{ref} - y) - \delta_a \quad (44)$$

$$\dot{y} = \frac{1}{T_{cp}}\frac{(U_0 - 2Rx_4 + Rx_3 + \Delta U)}{U_0 - 2Rx_4 + Rx_3}(y_{ref} - y) - \tilde{\delta}_b \quad (45)$$

A deviation in the voltage model results in a variation of

the controller time constant (44), (45) and does not change the property to reach the correct steady state power as the time derivative of x_3 still vanishes over time.

IV. Simulation Results

The simulation model is developed and run in Matlab/Simulink®. The nonlinear electrical power controller was simulated with the nonlinear fuel cell system model. The step-like power request is shown in figure 4 and was requested for a high and low cathode stoichiometry in order to operate the fuel cell system at different stack temperatures and cathode pressures to test the controller's robustness against model uncertainties. The heat exchanger cooling fan was run at constant speed.

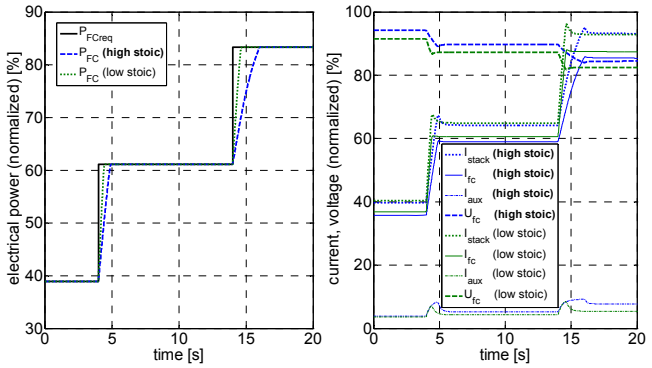

Fig. 4. Simulation results (left) of the nonlinear controller and the fuel cell system model: power request (black line), electrical power at high stoich. (blue) and at low stoich. (green); *right*: fuel cell current (solid line), stack current (dotted line), auxiliary current (dashed, dotted line) and voltage (dashed line) at high (blue) and at low stoich. (green); normalized values

As shown in figure 4 dynamics of the electrical power control is prescribed by the fuel cell system dynamics. Due to the internal fuel cell system control, the controller can maximally be as fast as the internal control. As shown in figure 4, auxiliary current settles at a constant value showing that its derivative goes to zero over time resulting in the correct steady state value for the fuel cell system power. The compressor's power consumption when providing a higher mass flow at higher stoichiometries results in a higher auxiliary current. Also, at high stoichiometries the overall system dynamics decreases as the compressor takes longer to provide the higher mass flow as requested (figure 4). Differences in stack temperature and pressure cause a variation in stack voltage when stack current is kept constant and therefore causes parameter uncertainties of the power controller model. However, the controller copes with these uncertainties and controls for the electrical power requested.

V. Conclusion

A self-powered Intelligent Energy® fuel cell system model with an internal fuel cell system controller has been derived and modeled in Matlab/Simulink®. The fuel cell system is electrically connected to an ohmic electronic load. A nonlinear power controller with proportional like structure is proposed based on a feedback-linearization approach and a simplified fuel cell system model with a linear polarization curve. The controller has been implemented in the nonlinear simulation model. Simulations show clearly that the controller works properly even if the plant voltage model deviates from the model for controller design.

References

[1] E. Vredenborg, H. Lüdders and F. Thielecke, "Methodik zur Auslegung und Simulation komplexer Brennstoffzellensysteme", *Deutscher Luft- und Raumfahrtkongress 2010*, DocumentID: 161248.

[2] J. Bleil, "Brennstoffzellen zur Bordstromversorgung von Flugzeugen", *HZwei-Das Magazin für Wasserstoff und Brennstoffzellen*, 04/2007

[3] Borup, R. (2007). Scientific Aspects of Polymer Electrolyte Fuel Cell Durability and Degradation. *Chem. Rev.*, **107**, 3904-3951.

[4] P. Adcock, A. Kells and C. Jackson, "PEM Fuel Cells for Road Vehicles", *EET-2008 European Ele-Drive Conference*, International Advanced Mobility Forum, Geneva Switzerland, 2008.

[5] Real, del A.J., Arce, A. and Bordons, C. (2007). Development and experimental validation of a PEM fuel cell dynamic model. *Journal of Power Sources*, **173**, 310-324

[6] J. T. Pukrushpan, A. G. Stefanopoulou and H. Peng, *Control of Fuel Cell Power Systems*. London: Springer-Verlag, 2004.

[7] M. Schultze, J. Horn, "A Control Oriented Simulation Model of an Evaporation Cooled Polymer Electrolyte Membrane Fuel Cell System", 18th IFAC World Congress, 2011

[8] M. Schultze, J. Horn, "Current Control of a PEMFC System connected to an Electrical Load through a DC/DC Converter", MED 2011, 2011

[9] Karnik, A.Y., Sun, J. Stefanopoulou, A.G. and Buckland J.H. (2009). Humidity and Pressure Regulation in a PEM Fuel Cell Using a Gain-Scheduled Static Feedback Controller. *IEEE Transactions on Control Systems Technology*, **17**, No. 2, 283-297

[10] M. H. Nehrir and C. Wang, *Modeling and Control of Fuel Cells*. Hoboken, NJ: John Wiley & Sons, 2009.

[11] P. Rodatz, G. Paganelli, L. Guzella, "Optimizing Air Supply Control of a Fuel Cell System", ACC 2003

[12] A. Arce, D. R. Ramirez, A. J. del Real and C. Bordons, "Constrained Explicit Predictive Control Strategies for PEM Fuel Cell Systems", Proceedings of the 46th IEEE Conference on Decision and Control, 2007

[13] J. Niemeyer, *Modellprädiktive Regelung eines PEM-Brennstoffzellensystems*, Schriften des Instituts für Regelungs- und Steuerungssysteme, Universität Karlsruhe, Band 05

[14] Q. Li, W. Chen, Y. Wang, J. Jia and M. Han, "Nonlinear robust control of proton exchange membrane fuel cell by state feedback exact linearization", Journal of Power Sources, 194, 338-348, 2009

[15] W. K. Na, B. Gou, "Feedback-Linearization-Based Nonlinear Control for PEM Fuel Cells", IEEE Transactions on Energy Conversion, vol 23, No. 1, 2008

[16] H. D. Baehr and S. Kabelac, *Thermodynamik*, Berlin: Springer-Verlag, 2006

[17] Navarro, H.A. and Cabezas-Gómez, L.C. (2007). Effectiveness-NTU Computation with a Mathematical Model for Cross-Flow Heat Exchangers. *Brazilian Journal of Chemical Engineering*, **24**, 509-521.

[18] J. C. Amphlett, R. M. Baumert, R. F. Mann, B. A. Peppley and P. R. Roberge, "Performance Modeling of the Ballard Mark IV Solid Polymer Electrolyte Fuel Cell", *J. Electrochem. Soc.*, vol. 142, pp. 1-8, 1995

[19] R. O'Hayre, S.-W. Cha, W. Colella and F. B. Prinz, *Fuel Cell Fundamentals*. Hoboken, NJ: John Wiley & Sons, 2009.

[20] A. Lücken, M. Schultze, J. Horn, D. Schulz, "Analysis of different Methods to Improve the Fuel Cell Dynamics for Modern Aircraft Applications", UPEC 2011, 2011